Monthly Notices
of the
ROYAL ASTRONOMICAL SOCIETY
MNRAS **490,** 1638–1643 (2019) doi:10.1093/mnras/stz2743

Coexistence of a planar magnetic structure and an Alfvén wave in the shock-sheath of an interplanetary coronal mass ejection

Zubair I. Shaikh [1]★ Anil Raghav [2] and Geeta Vichare[1]

[1]*Indian Institute of Geomagnetism (IIG), New Panvel, Navi Mumbai-410218, India*
[2]*Department of Physics, University of Mumbai, Vidyanagari, Santacruz (E), Mumbai-400098, India*

Accepted 2019 September 26. Received 2019 July 29; in original form 2019 January 10

ABSTRACT

The excess speed of coronal mass ejection over the ambient solar wind in interplanetary space generates a highly compressed, heated and turbulent shock-sheath. Here, for the first time, we present *in situ* observations of a unique and distinct feature of the shock-sheath, which exhibits the characteristics of a planar magnetic structure (PMS) and an Alfvén wave simultaneously. We have used standard techniques to confirm the presence of the PMS as described in Shaikh et al. We have employed the minimum variance analysis technique to estimate the properties of the PMS. The Walén test is used to confirm the presence of the Alfvén wave. Our study unambiguously proves the coexistence of the Alfvén wave and the PMS in the shock-sheath region. Further studies are essential to investigate the origin of such a peculiar shock-sheath and its effect on our view of solar-terrestrial physics.

Key words: MHD – turbulence – Sun: coronal mass ejections (CMEs) – solar wind .

1 INTRODUCTION

Interplanetary coronal mass ejections (ICMEs) are large-scale magnetic structures in interplanetary space that can be described as loops or bubble-like in nature (Gosling, Pizzo & Bame 1973; Palmer, Allum & Singer 1978). They carry solar coronal plasma (Low 1996) and can cause extreme space weather conditions near the Earth and other planets. They also pose hazards for spacecraft throughout the heliosphere. Thus, studies of ICMEs are significant from both scientific and technological points of view (Schwenn 2006; Moldwin 2008). Extensive studies in the last few decades have reported that an ICME has two major substructures: a shock-sheath and a magnetic cloud (MC; Burlaga et al. 1981, 2001; Burlaga, Lepping & Jones 1990; Lepping et al. 1997; Zurbuchen & Richardson 2006; Richardson & Cane 2010). The shock-sheath of an ICME has a highly turbulent, compressed nature and associated structures, and also high values of parameters such as temperature, plasma density and plasma beta (Zurbuchen & Richardson 2006; Kilpua, Koskinen & Pulkkinen 2017). Therefore, a detailed investigation of these structures is essential for understanding the coupling of solar wind and the magnetosphere.

The ICME triggers several physical phenomena observed on Earth, such as geomagnetic storms (Gonzalez & Tsurutani 1987; Gonzalez et al. 1994; Lepping et al. 1997; Akasofu 2011; Raghav et al. 2018), Forbush decreases (Lockwood 1971; Cane 2000; Raghav et al. 2014, 2017; Bhaskar et al. 2016) and auroras (Baker & Lanzerotti 2016). A shock-sheath is most geo-effective during the ascending and maximum phases of the solar cycle (Richardson & Cane 2012). Moreover, it is responsible for particle acceleration in space (e.g. solar energetic particle events), auroral current systems and depletions of electron fluxes in the radiation belt (Baker et al. 1996; Huttunen & Koskinen 2004; Kilpua et al. 2013a, 2015, 2017; Hietala et al. 2014; and references therein). The high-energy electron flux in the radiation belt is the key to climate models, the understanding of atmospheric chemistry and the corresponding climatological effects (Verronen et al. 2011; Andersson et al. 2014; Seppälä et al. 2014; Mironova et al. 2015).

Until now, only a few studies have found plasma waves or a substructure within the shock-sheath. Recently, there have been observations indicating the presence of mirror mode waves (Liu et al. 2006), ultra-low frequency (ULF) waves (0.01–0.05 Hz; Kilpua et al. 2013b), magnetic field fluctuations of large amplitude, intense irregular ULF fluctuations and regular high-frequency (HF) wave activity ($\geq$ 1 Hz; Kataoka et al. 2005; Kajdič et al. 2012) within the shock-sheath. Further, Kataoka et al. (2005) and Feng & Wang (2013) reported plasma discontinuities and reconnection exhausts in a shock-sheath region. Besides, substructures such as the plasma depletion layer (a high-density plasma region), the pile-up compression region (a low-density plasma region; Erkaev et al. 1995; Farrugia et al. 1997; Liu et al. 2006; Das et al. 2011) and the small-scale flux-rope (Shaikh, Raghav & Bhaskar 2017) have also been identified within the shock-sheath. In addition, these structures can be seen in the planetary magnetosphere as well as in interplanetary space (Zwan & Wolf 1976; Moldwin et al. 2000; Slavin et al. 2003; Cartwright & Moldwin 2008, 2010; Hu et al. 2014; Zheng & Hu 2016).

Other than small-scale flux-ropes, a planar magnetic structure (PMS) has also been observed in interplanetary space (Nakagawa,

★ E-mail: zubairshaikh584@gmail.com

Nishida & Saito 1989; Nakagawa 1993; Neugebauer, Clay & Gosling 1993; Hakamada 1998; Jones, Balogh & Horbury 1999). The PMS evolves in the shock-sheath region, which can enhance its geo-effectiveness (Kataoka et al. 2015; Palmerio, Kilpua & Savani 2016). It has been suggested that Alfvén waves are responsible for the long recovery phase of the corotating interaction region (Tsurutani et al. 2006, 2011; Zhang et al. 2014) or the ICME-induced geomagnetic storm (Raghav et al. 2018; Raghav, Chorghe & Shaikh 2019). Moreover, Shaikh et al. (2018) have reported the existence of a PMS within the trailing edge of the shock-sheath, where it causes a decrease in the flux of galactic cosmic rays. In addition, a shock-sheath provides a unique opportunity to study the features of plasma turbulence and energy dissipation. Further, the first observation of Alfvénic shock has been reported, and the possible implications are discussed by Raghav & Shaikh (2018). The high compression between the shock front and the leading edge of the magnetic cloud can cause instability or anisotropy in the incompressible plasma system, which might trigger different types of waves or structures. This is a motivation to look for basic incompressible MHD fluctuations, namely magnetosonic (fast), Alfénic (intermediate) and sonic (slow) waves in the shock-sheath region. To the best of our knowledge, here we demonstrate for the very first time a shock-sheath with the unique feature of exhibiting simultaneous characteristics of a PMS and Alfvén wave.

2 EVENT DETAILS

The studied shock-sheath event is caused by the CME that crossed the *Wind* satellite on 2000 October 12. During the crossing of the CME, the position of the *Wind* satellite (in terms of R_e) in GSE coordinates was $x = 31.11$, $y = -239.73$, $z = -0.64$. This implies that *Wind* was not near L1 at the time; it was outside the magnetosphere and off to the side. The temporal variations of the magnetic field and various plasma parameters are shown in Fig. 1. We have used *in situ* data from the *Wind* data base[1] with 92-s resolution. The arrival of the shock front is identified as a sudden sharp enhancement in the interplanetary magnetic field (IMF) parameters: B_{mag}, V_p, T and N_p (see the first vertical black dashed line). Various characteristics of the shock can be obtained from the Harvard Smithsonian Center for Astrophysics Interplanetary Shock Database data base.[2] The shock front is followed by high N_p, T, V_p and β, large fluctuations in B_{comp} and enhanced magnetic field strength, which is demonstrated as the shock-sheath region of the ICME (the first shaded region in Fig. 1; Shaikh et al. 2017). The shock-sheath lasts about ∼19 h. Furthermore, the second shaded region shows the minimum fluctuations in B_{mag} and B_{comp}, the slow variation in θ and ϕ, and the slow, steady trend in V_p and low β. This region is manifested as a magnetic cloud of CME (Zurbuchen & Richardson 2006). The boundary of the MC is supported by the catalogue available at the DREAMS web site (Chi et al. 2016).[3]

3 DATA ANALYSIS

The minimum variance analysis (MVA) technique is utilized for the IMF data to investigate the features of the shock-sheath region.

[1] Available at https://wind.nasa.gov/mfi_swe_plot.php.
[2] See https://www.cfa.harvard.edu/shocks/wi_data/00179/wi_00179.html.
[3] See http://space.ustc.edu.cn/dreams/wind_icmes/, which is generated and maintained by the Solar-Terrestrial Exploration and Physics (STEP) team at the University of Science and Technology of China (USTC).

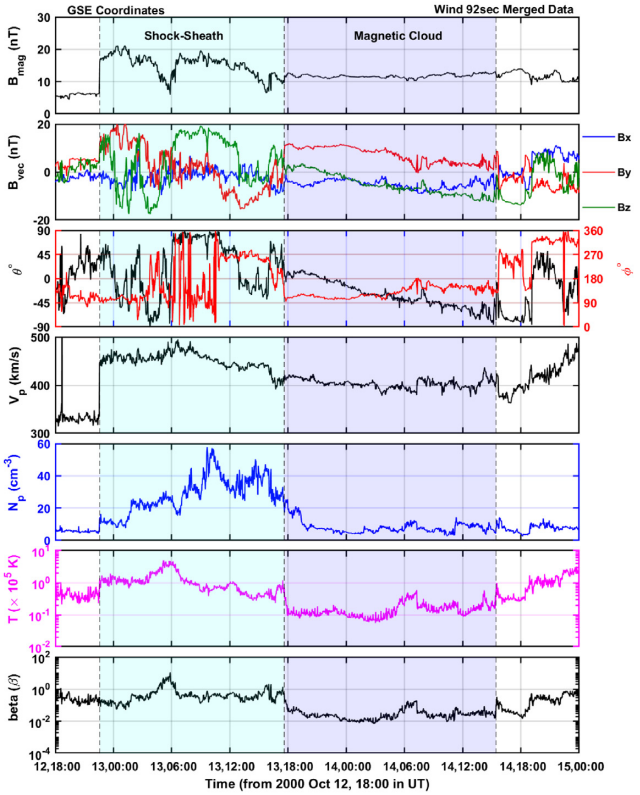

Figure 1. ICME observed by the *WIND* spacecraft on 2000 October 12–14 at 1 au. The top two panels show the temporal variation of the IMF B_{mag} and B_{vec} (i.e. B_X, B_Y and B_Z). The third panel represents the azimuth ϕ and elevation θ angles of the IMF vector. The fourth and fifth panels show solar wind speed V_p and plasma density N_p.The sixth and seventh panels give the temporal evolution of temperature ($T_p = \times 10^5$ K) and plasma beta β, respectively. The sudden commencement of the shock is shown by the first vertical black dashed line. The shock-sheath and MC regions are shown by different coloured shading.

The output of the MVA gives three eigenvalues (λ_1, λ_2 and λ_3) in descending order and the corresponding eigenvectors ($\vec{e_1}$, $\vec{e_2}$ and $\vec{e_3}$). Note that B_1^*, B_2^* and B_3^* are IMF vectors after the MVA analysis corresponding to the maximum, intermediate and minimum variance directions (Sonnerup & Scheible 1998). These values are used for the identification of the PMS and to study the characteristics of the Alfvén wave.

3.1 PMS identification

For the identification of the PMS, we employed the method discussed by Shaikh et al. (2018) and references therein. A structure is said to be planar if the following criteria are satisfied: a wide distribution of the ϕ angle, $0^\circ < \phi < 360^\circ$; good planarity (confirmation of the two dimensions), $|B_n|/B \leq 0.2$; good efficiency (of the MVA technique) $R = \lambda_2/\lambda_3 \geq 3$ (Nakagawa et al. 1989; Palmerio et al. 2016).

Fig. 2 demonstrates the distribution of the magnetic field orientation (i.e. θ and ϕ within the shock-sheath region). It is consistent with the expected distribution (a wave-like pattern) of a typical PMS (see the fitted model curve in Fig. 2), which suggests the possible existence of a PMS. The estimated planarity ($|B_n|/\langle B\rangle$) and efficiency (λ_2/λ_3) associated with the studied region are 0.20 and 10.99, respectively. This explicitly confirms that the shock-sheath region

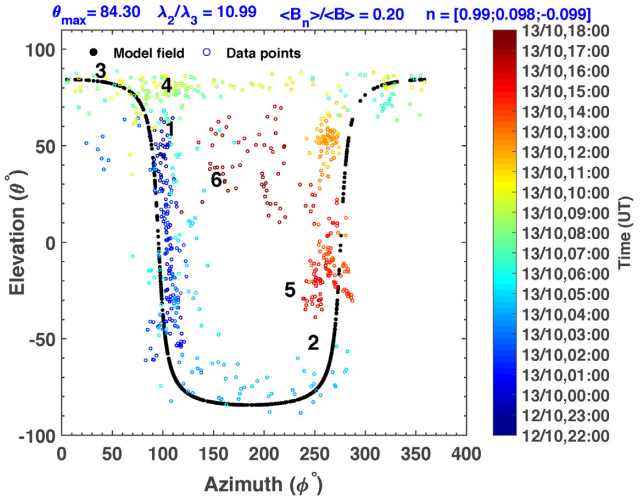

Figure 2. The $\phi-\theta$ distribution of the shock-sheath region, where ϕ and θ are the azimuthal and elevation angles of the magnetic field vector, respectively. The angular distribution of the model field is shown by the black curve. The colour bar gives the temporal evolution of the $\phi-\theta$ distribution. In the PMS plane, the IMF vectors are parallel and contain the spiral direction (i.e. at $\theta = 0°$, we obtain $\sim\phi = 95.^{\circ}71$ and $\sim\phi = 275.^{\circ}5$). θ_{max} is the PMS plane inclination with respect to the ecliptic plane. The numbers 1 to 6 denote Alfvén wave arc polarization points.

evolves as a PMS structure (Nakagawa et al. 1989; Neugebauer et al. 1993; Jones et al. 1999). Moreover, the PMS plane has an inclination of $\theta_{max} = 84.^{\circ}2976$ with respect to the ecliptic plane and the normal vector to the PMS plane is $\boldsymbol{n} = (0.990, 0.098, -0.099)$. At $\theta = 0$, the PMS plane intersects at $\sim\phi = 95.^{\circ}71$ and $275.^{\circ}5$, which implies that the Archimedean spiral direction is included in the plane (Nakagawa 1993; Jones et al. 1999; Kilpua et al. 2017). The average magneto-sonic Mach number (M_{ms}) and Alfvénic Mach number (M_A) in the PMS are ~5.72 and ~7.76, respectively. For the PMS observed in the 2-h downstream region of the shock, statistical studies indicate the limits of the above parameters as $M_{ms} > 2.5$ and $M_A > 2$. In fact, it is emphasized that the PMS will be absent if $M_A < 2.0$ and $\beta < 0.05$ (Kataoka et al. 2005). In the present study, $\beta = 0.65$, which is clearly well above the stated criterion, $\beta > 0.05$ (see Fig. 1); thus, the studied shock-sheath region satisfies all the criteria for a PMS.

3.2 Alfvén wave identification

In Alfvén waves, the plasma fluid velocity and magnetic field perturbations are perpendicular to a magnetic tension force, which is along the direction of the resultant magnetic field. The Alfvén velocity is represented as

$$V_A = \pm A \frac{B}{\sqrt{\mu_0 \rho}} \qquad (1)$$

$$A = \sqrt{1 - \frac{\mu_0 (P_{\parallel} - P_{\perp})}{B^2}},$$

where ρ, B, A, $P_{\parallel}$, $P_{\perp}$ and $\pm$ are proton mass density, magnetic field vector, thermal anisotropy parameter (= 1 at 1 au), thermal pressure parallel and perpendicular to B_0, and the wave propagation direction antiparallel or parallel to the background magnetic field B_0, respectively (Burlaga 1971; Yang et al. 2016). Thus, a good correlation between the change in the magnetic field and plasma velocity is expected. This is represented in terms of the Walén

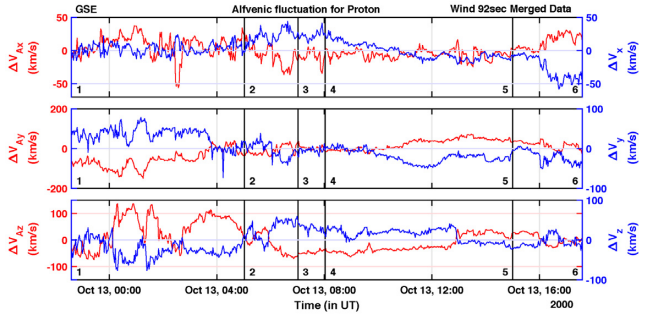

Figure 3. The temporal variation of the Alfvén velocity fluctuation vector ΔV_A (red) and that of the proton flow velocity fluctuation vector ΔV (blue). The black vertical lines (1–6) denote the arc polarization portion of the Alfvén wave (see Fig. 4).

relation (Walén 1944; Hudson 1971) as

$$\Delta V_A = \frac{\Delta B}{\sqrt{\mu_0 \rho}} \qquad (2)$$

$$\Delta V = |R_W| \Delta V_A,$$

where $\Delta B = B - B_{avg}$ and $\Delta V = V - V_{avg}$. The correlation between the ΔV and ΔV_A components gives the information about the presence of the Alfvén wave. The Walén slope (R_W) gives the linear relationship between ΔV and ΔV_A (Burlaga 1971; Yang et al. 2016; Raghav & Kule 2018; Raghav et al. 2018).

A visual inspection of Fig. 3 clearly shows that the x, y and z components of ΔV and ΔV_A are negatively correlated. The estimated Pearson correlation coefficients (R) along the x, y and z directions are −0.52, −0.85 and −0.82, and the regression coefficients (slope of the fit) are −0.63, −0.53 and −0.44, respectively (this plot is not shown here), which indicates the existence of an Alfvén wave in the studied shock-sheath region (Lepping et al. 1997; Yang et al. 2016). The strong negative correlations between ΔV_{Ax} and ΔV_x, ΔV_{Ay} and ΔV_y and ΔV_{Az} and ΔV_z indicate the propagation of the Alfvén wave towards the Sun (Gosling, Teh & Eriksson 2010; Zhang et al. 2014).

4 DISCUSSION AND CONCLUSION

The studied shock-sheath region clearly depicts the simultaneous existence of a PMS (see Fig. 2) and an Alfvén wave (see Fig. 3). The existence of a PMS shows that all magnetic field vectors in the shock-sheath region are in a plane and have different orientations. The estimated thickness of the PMS/shock-sheath is about 0.21 au, which is calculated by multiplying the average solar wind velocity (~450 km s^{-1}) with total time duration (~19.5 h). The origin of the PMS might be: (i) the compression of plasma by fast streams (Neugebauer et al. 1993); (ii) sector boundary crossings; (iii) draping of magnetic field lines about a magnetic structure (Farrugia et al. 1990); (iv) the propagation of a fast shock and the alignment of pre-existing discontinuities caused by the passage of a shock (Neugebauer et al. 1993; Jones et al. 1999; Palmerio et al. 2016). It is believed that the compression is the main criterion for the origin of the PMS in interplanetary space. Nakagawa (1993) found no significant correlation between the PMS and solar wind speed during filament or flare eruptions, which indicates that the Sun is not a source of the PMS. However, observations of the PMS at the same heliospheric longitude in successive rotations of the Sun indicate that the origin of the PMS could be on the Sun (Nakagawa 1993). Generally, compression is a major mechanism for the generation of a PMS (Nakagawa 1993; Neugebauer et al.

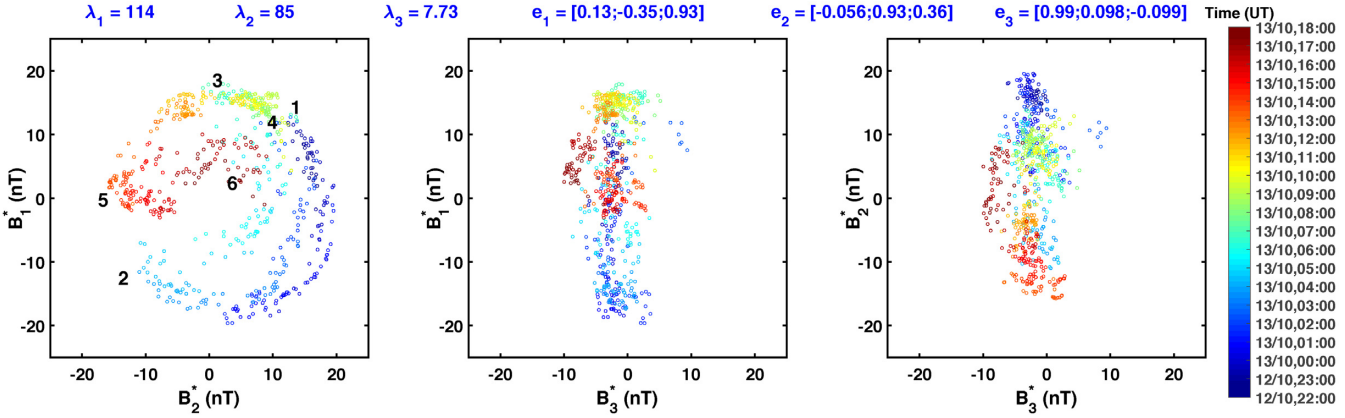

Figure 4. Hodogram plot of the ICME shock-sheath region, where B_1^*, B_2^* and B_3^* are the magnetic field vectors after MVA analysis.

1993; Palmerio et al. 2016). The high Mach number in the studied region can be associated with high ion densities and a high magnetic field. The increased density at the middle can be correlated with the compressed region called the pile-up compression region. Therefore, we suggest that the PMS originates either as a result of compression with the lateral expansion of the region by the ICME or the draping of the plasma around the MC surface, or it was already present in the solar wind and dragged by the CME in interplanetary space (Nakagawa 1993; Neugebauer et al. 1993; Palmerio et al. 2016). Conclusively, there is a discrepancy about the origin of the PMS.

After performing the MVA technique, the hodogram analysis (see Fig. 4) is used to study the features of the observed Alfvén wave towards the Sun. In Fig. 3, we observe a 720° cycle of an Alfvén wave, which is indicated by vertical lines from 1 to 6; we can identify the start of the wave at 1 and the end of the wave at 6. The projection in the B_1^* and B_2^* plane demonstrates the time evolution of the Alfvén wave, which indicates that the wave starts at one point, completes a half circle and then returns to the starting point. This type of feature of the wave is called arc polarization (Riley et al. 1995, 1996; Tsurutani et al. 1995). It also indicates that the wave does not have a steady rate of wave phase rotation with time; this indicates phase-steepened phenomena. For each arc, there is a ∼180° phase rotation, from 1 to 2, 2 to 3, 4 to 5 and 5 to 6 (see Fig. 4). The point 1 to 2 is the initial portion of the wave and the 5 to 6 point represents the trailing portion of the wave carrying the phase rotation (half-circle). Therefore, the wave period is doubled two times, suggesting a period-doubling phenomenon. A detailed understanding of these characteristics of Alfvén waves is discussed in Tsurutani et al. (2018) and references therein. Observations of Alfvén waves towards the Sun are very rare in the solar wind (Belcher, Davis & Smith 1969; Belcher & Davis 1971; Burlaga & Turner 1976; Denskat & Neubauer 1982; Riley et al. 1996; Yang et al. 2016). The origin of the Alfvén wave might be: (i) velocity shear instabilities (Coleman 1968; Bavassano, Dobrowolny & Moreno 1978; Roberts et al. 1992); (ii) kinetic instabilities associated with the solar wind proton heat flux (Goldstein et al. 2000; Matteini et al. 2013); (iii) the steepening of a magnetosonic wave, which forms the shock at the leading edge of the magnetic cloud (Tsurutani et al. 1988, 2011); (iv) the oblique firehose instability (Matteini et al. 2006, 2007; Hellinger & Trávníček 2008); (v) the interaction of multiple CMEs (Raghav & Kule 2018). In general, the CME shock-sheath does not exhibit Alfvénic characteristics. This type of event is unique or rare to observe. Therefore, we suggest that the exceptional feature of PMS evolution within the shock-sheath may trigger plasma instability, which could be responsible for Alfvén wave generation in the shock-sheath region.

5 IMPLICATION

Recent studies suggest that high compression may decrease the perpendicular diffusion coefficient during the random walk of field lines, which might result in the decrease in cosmic ray intensity (Intriligator & Siscoe 1995; Intriligator et al. 2001). Cosmic rays interact with Alfvén waves either adiabatically through magnetic mirror scattering or non-adiabatically through gyro-frequency resonance (Kulsrud & Pearce 1969; Holmes & Sciama 1975). Therefore, it is very intriguing to study the cosmic ray response to the identified shock-sheath. Besides this, drivers of a significant magnetic storm can be either a strong southward magnetic field (B_z) along with high compression in the PMS causing less adiabatic expansion, or a pile-up of plasma in front of the MC, higher than usual, accompanied with the strong magnetic field, and high density in the shock-sheath region (Kataoka et al. 2015). Moreover, Alfvén waves control the dynamics of geomagnetic storms and extend the recovery time (Tsurutani et al. 1995, 2011; Raghav et al. 2018). Therefore, the geomagnetic storm corresponding to the studied event is also exciting, and it will be the future direction of our investigation. Besides, the shock-sheath has significant effects on other planets and their atmospheres, such as loss of ion flux (>9 amu) from Mars (Jakosky et al. 2015). Thus, the typical features of a shock sheath, its origin and its influence in association with solar-terrestrial physics need further detailed study.

ACKNOWLEDGEMENTS

The authors are thankful to Lynn B. Wilson and the Wind instrument teams for making interplanetary data available. Z.S. is also thankful to Ms. Gauri Datar for their help to improve the manuscript grammatically correct. Authors would like to thanks the anonymous referee for there valuable suggestion which improves the manuscript.

REFERENCES

Akasofu S.-I., 2011, Space Science Reviews, 164, 85
Andersson M., Verronen P., Rodger C., Clilverd M., Seppälä A., 2014, Nature Communications, 5, 5197

Baker D. N., Lanzerotti L. J., 2016, American Journal of Physics, 84, 166
Baker D. N., Pulkkinen T., Angelopoulos V., Baumjohann W., McPherron R., 1996, J. Geophys. Res.: Space Physics, 101, 12975
Bavassano B., Dobrowolny M., Moreno G., 1978, Solar Physics, 57, 445
Belcher J., Davis L., Jr., 1971, J. Geophys. Res., 76, 3534
Belcher J., Davis L., Jr., Smith E., 1969, J. Geophys. Res., 74, 2302
Bhaskar A., Vichare G., Arunbabu K., Raghav A., 2016, Ap&SS, 361, 242
Burlaga L. F., 1971, J. Geophys. Res., 76, 4360
Burlaga L., Turner J., 1976, J. Geophys. Res., 81, 73
Burlaga L., Sittler E., Mariani F., Schwenn R., 1981, J. Geophys. Res.: Space Physics, 86, 6673
Burlaga L., Lepping R., Jones J., 1990, in Russell C. T., Priest E. R., Lee L. C.(eds), Physics of Magnetic Flux Ropes. American Geophysical Union, Washington, DC, p. 373
Burlaga L., Skoug R., Smith C., Webb D., Zurbuchen T., Reinard A., 2001, J. Geophys. Res.: Space Physics, 106, 20957
Cane H. V., 2000, Space Science Reviews, 93, 55
Cartwright M., Moldwin M., 2008, J. Geophys. Res.: Space Physics, 113, A09105
Cartwright M., Moldwin M., 2010, J. Geophys. Res.: Space Physics, 115, A10110
Chi Y., Shen C., Wang Y., Xu M., Ye P., Wang S., 2016, Solar Physics, 291, 2419
Coleman P. J., Jr., 1968, ApJ, 153, 371
Das I., Opher M., Evans R., Loesch C., Gombosi T. I., 2011, ApJ, 729, 112
Denskat K., Neubauer F., 1982, J. Geophys. Res.: Space Physics, 87, 2215
Erkaev N., Farrugia C., Biernat H., Burlaga L., Bachmaier G., 1995, J. Geophys. Res.: Space Physics, 100, 19919
Farrugia C., Dunlop M., Geurts F., Balogh A., Southwood D., Bryant D., Neugebauer M., Etemadi A., 1990, Geophys. Res. Lett., 17, 1025
Farrugia C., Erkaev N., Biernat H., Burlaga L., Lepping R., Osherovich V., 1997, J. Geophys. Res, 102, 7089
Feng H., Wang J., 2013, A&A, 559, A92
Goldstein B. E., Neugebauer M., Zhang L. D., Gary S. P., 2000, Geophys. Res. Lett., 27, 53
Gonzalez W. D., Tsurutani B. T., 1987, Planetary and Space Science, 35, 1101
Gonzalez W., Joselyn J. A., Kamide Y., Kroehl H. W., Rostoker G., Tsurutani B., Vasyliunas V., 1994, J. Geophys. Res.: Space Physics, 99, 5771
Gosling J. T., Pizzo V., Bame S. J., 1973, J. Geophys. Res., 78, 2001
Gosling J., Teh W-L., Eriksson S., 2010, ApJ, 719, L36
Hakamada K., 1998, Solar Physics, 181, 73
Hellinger P., Trávníček P. M., 2008, J. Geophys. Res.: Space Physics, 113, A10109
Hietala H., Kilpua E., Turner D., Angelopoulos V., 2014, Geophys. Res. Lett., 41, 2258
Holmes J. A., Sciama D., 1975, MNRAS, 170, 251
Hu Q., Qiu J., Dasgupta B., Khare A., Webb G., 2014, ApJ, 793, 53
Hudson P., 1971, Planetary and Space Science, 19, 1693
Huttunen K., Koskinen H., 2004, Annales Geophysicae, 22, 1729
Intriligator D. S., Siscoe G. L., 1995, J. Geophys. Res.: Space Physics, 100, 21605
Intriligator D., Jokipii J., Horbury T., Intriligator J., Forsyth R., Kunow H., Wibberenz G., Gosling J., 2001, J. Geophys. Res.: Space Physics, 106, 10625
Jakosky B. M. et al., 2015, Science, 350, 0210
Jones G., Balogh A., Horbury T., 1999, Geophys. Res. Lett., 26, 13
Kajdič P., Blanco-Cano X., Aguilar-Rodriguez E., Russell C., Jian L., Luhmann J., 2012, J. Geophys. Res.: Space Physics, 117, A06103
Kataoka R., Watari S., Shimada N., Shimazu H., Marubashi K., 2005, Geophys. Res. Lett., 32
Kataoka R., Shiota D., Kilpua E., Keika K., 2015, Geophysical Research Letters, 42, 5155
Kilpua E., Isavnin A., Vourlidas A., Koskinen H., Rodriguez L., 2013a, Annales Geophysicae, 31, 1251
Kilpua E., Hietala H., Koskinen H., Fontaine D., Turc L., 2013b, Annales Geophysicae, 31, 1559
Kilpua E. et al., 2015, Geophysical Research Letters, 42, 3076
Kilpua E., Koskinen H. E., Pulkkinen T. I., 2017, Living Reviews in Solar Physics, 14, 5
Kulsrud R., Pearce W. P., 1969, ApJ, 156, 445
Lepping R. et al., 1997, J. Geophys. Res.: Space Physics, 102, 14049
Liu Y., Richardson J., Belcher J., Kasper J., Skoug R., 2006, J. Geophys. Res.: Space Physics, 111, A09108
Lockwood J. A., 1971, Space Science Reviews, 12, 658
Low B., 1996, Solar Physics, 167, 217
Matteini L., Landi S., Hellinger P., Velli M., 2006, J. Geophys. Res.: Space Physics, 111, A10101
Matteini L., Landi S., Hellinger P., Pantellini F., Maksimovic M., Velli M., Goldstein B. E., Marsch E., 2007, Geophys. Res. Lett., 34, L20105
Matteini L., Hellinger P., Goldstein B. E., Landi S., Velli M., Neugebauer M., 2013, J. Geophys. Res.: Space Physics, 118, 2771
Mironova I. A. et al., 2015, Space Science Reviews, 194, 1
Moldwin M., 2008, An Introduction to Space Weather. Cambridge University Press, Cambridge
Moldwin M., Ford S., Lepping R., Slavin J., Szabo A., 2000, Geophys. Res. Lett., 27, 57
Nakagawa T., 1993, Solar Physics, 147, 169
Nakagawa T., Nishida A., Saito T., 1989, J. Geophys. Res.: Space Physics, 94, 11761
Neugebauer M., Clay D., Gosling J., 1993, J. Geophys. Res.: Space Physics, 98, 9383
Palmer I., Allum F., Singer S., 1978, J. Geophys. Res.: Space Physics, 83, 75
Palmerio E., Kilpua E. K., Savani N. P., 2016, Ann. Geophys, 34, 313
Raghav A. N., Kule A., 2018, MNRAS, 476, L6
Raghav A. N., Shaikh Z. I., 2018, preprint (arXiv:1810.06004)
Raghav A., Bhaskar A., Lotekar A., Vichare G., Yadav V., 2014, Journal of Cosmology and Astroparticle Physics, 2014, 074
Raghav A., Shaikh Z., Bhaskar A., Datar G., Vichare G., 2017, Solar Physics, 292, 99
Raghav A. N., Kule A., Bhaskar A., Mishra W., Vichare G., Surve S., 2018, ApJ, 860, 26
Raghav A. N., Choraghe K., Shaikh Z. I., 2019, MNRAS, 488, 910
Richardson I., Cane H., 2010, Solar Physics, 264, 189
Richardson I. G., Cane H. V., 2012, Journal of Space Weather and Space Climate, 2, A01
Riley P., Sonett C., Balogh A., Forsyth R., Scime E., Feldman W., 1995, Space Science Reviews, 72, 197
Riley P., Sonett C., Tsurutani B., Balogh A., Forsyth R., Hoogeveen G., 1996, J. Geophys. Res.: Space Physics, 101, 19987
Roberts D. A., Goldstein M. L., Matthaeus W. H., Ghosh S., 1992, J. Geophys. Res.: Space Physics, 97, 17115
Schwenn R., 2006, Living Reviews in Solar Physics, 3, 2
Seppälä A., Matthes K., Randall C. E., Mironova I. A., 2014, Progress in Earth and Planetary Science, 1, 24
Shaikh Z., Raghav A., Bhaskar A., 2017, ApJ, 844, 121
Shaikh Z. I., Raghav A. N., Vichare G., Bhaskar A., Mishra W., 2018, ApJ, 866, 118
Slavin J. et al., 2003, J. Geophys. Res.: Space Physics, 108, 1015
Sonnerup B. U., Scheible M., 1998, in Götz P., Daly P.(eds), ISSI Scientific Reports Series, Vol. 1, Analysis Methods for Multi-Spacecraft Data, International Space Science Institute, Bern, p. 185
Tsurutani B. T., Gonzalez W. D., Tang F., Akasofu S. I., Smith E. J., 1988, J. Geophys. Res.: Space Physics, 93, 8519
Tsurutani B. T., Gonzalez W. D., Gonzalez A. L., Tang F., Arballo J. K., Okada M., 1995, J. Geophys. Res.: Space Physics, 100, 21717
Tsurutani B. T. et al., 2006, J. Geophys. Res.: Space Physics, 111, A07S01
Tsurutani B., Lakhina G., Verkhoglyadova O. P., Gonzalez W., Echer E., Guarnieri F., 2011, J. Atmos. Solar-Terrestrial Phys., 73, 5
Tsurutani B. T., Lakhina G. S., Sen A., Hellinger P., Glassmeier K.-H., Mannucci A. J., 2018, J. Geophys. Res.: Space Physics, 123, 2458

Verronen P. T., Rodger C. J., Clilverd M. A., Wang S., 2011, J. Geophys. Res.: Atmospheres, 116, D07307
Walén C., 1944, Arkiv for Astronomi, 30, 1
Yang L., Lee L., Chao J., Hsieh W., Luo Q., Li J., Shi J., Wu D., 2016, ApJ, 817, 178
Zhang X-Y., Moldwin M., Steinberg J., Skoug R., 2014, J. Geophys. Res.: Space Phys., 119, 3259
Zheng J., Hu Q., 2016, J. Phys.: Conf. Ser., 767, 012028
Zurbuchen T. H., Richardson I. G., 2006, in Kunow H.(ed.), Coronal Mass Ejections. Springer, Berlin, p. 31
Zwan B., Wolf R., 1976, J. Geophys. Res., 81, 1636

This paper has been typeset from a TEX/LATEX file prepared by the author.